Frequency Response of Avalanche Photodetectors with Separate Absorption and Multiplication Layers

Weishu Wu, Aaron R. Hawkins, and John E. Bowers

Abstract—**We present analytical expressions for the frequency response of avalanche photodetectors (APD's) with separate absorption and multiplication regions (SAM). The effect of the electric field profile in the multiplication layer on frequency response is considered for the first time. Previous theories have assumed that the multiplication layer is very thin and the peak electric field, which corresponds to the effective multiplication plane, is positioned away from the absorption layer. This is a poor assumption for many devices, and in particular for silicon hetero-interface photodetectors (SHIP's). We present a theoretical model in which the thickness of the multiplication layer is arbitrary and the peak electric field may be positioned arbitrarily in relation to the absorption layer. We also consider the effects of parasitics, transit-time, and avalanche buildup time. Both front and back illumination from either multiplication layer or absorption layer are considered. The calculated results are compared with experimental results for existing SHIP's and performance predictions are also made for optimized SHIP structures. SHIP APD's with gain-bandwidth product in excess of 500 GHz are possible.**

I. Introduction

AVALANCHE photodetectors (APD's) are useful for optical fiber communication systems operating near 1.3 or 1.55 μm [1]–[5] because APD receivers exhibit a higher sensitivity than PIN receivers due to the internal gain provided by APD's. Conventional InGaAs APD's have limited gain-bandwidth product and poor noise figure because of the small difference between hole and electron ionization coefficients in III-V semiconductors used to fabricate these detectors [6]–[7]. Si APD's are well known for low excess noise and high gain-bandwidth product due to the large difference of hole and electron ionization coefficients [8]. However, the quantum efficiency of Si APD's is negligible at 1.3–1.55 μm, making them unusable for fiber communication systems. To take advantage of the small excess noise of the multiplication process and high gain-bandwidth product and obtain high quantum efficiency, a structure based on fusing silicon to InGaAs has been proposed and demonstrated [5]. As shown in Fig. 1, Si is used as the multiplication material and InGaAs is used as the absorption material in the silicon hetero-interface photodetector (SHIP detector). The structure and/or the electric field profile in this APD is quite different from that of the existing Si APD's [9], [10] and InP/InGaAs APD's [11]–[13] and previous analytical expressions applicable to these earlier detectors are not accurate.

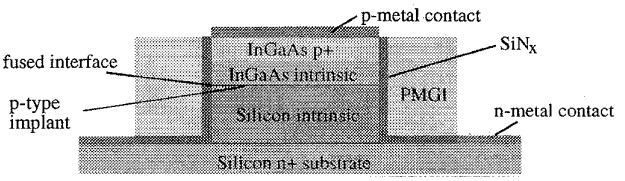

Fig. 1. Schematic drawing of the structure of a SHIP detector.

Previously, McIntyre [14] analyzed the frequency response of an APD with both electron and hole injection into the multiplication layer and Campbell *et al.* [11] presented a simple expression for the frequency response of an InP/InGaAs APD with only hole injection. This treatment is actually not valid for APD's with separate absorption and multiplication (SAM) structure. More recently, Campbell *et al.* [12] derived expressions of frequency response for a SAM–APD. This analysis was based on the assumptions that the multiplication layer was thin and the peak electric field (corresponding to the effective avalanche plane) was at the edge of the depletion layer, i.e., the interface of InP and the substrate. As a consequence, the contribution from the secondary major multiplying charges (holes in the case of InP/InGaAs APD's) to the photocurrent was neglected. As the multiplication layer gets thicker and/or the peak electric field shifts from the edge of the depletion layer, the contribution from the secondary multiplying charges can no longer be neglected. Other analyzes on the frequency response based on the approach of directly solving the carrier transport equations in the frequency domain [15] have also been presented by Hollenhorst [16] and Kahraman *et al.* [17]. Although these approaches [16]–[17] provide us a way of numerical calculation to take into account the effect of electric field profile on the frequency response, analytical expressions for both time and frequency response are difficult to obtain.

To obtain analytical expressions for time and frequency response of a SAM APD with arbitrary electric field profile, we use the concept of effective multiplication plane within the multiplication layer. This is a similar simplification for the multiplication process by assuming most of the multiplication occurs at that plane, which was previously assumed to be the edge of the depletion layer [12]. Effects of transit-time, para-

Manuscript received May 31, 1996; revised August 23, 1996. This work was supported by ARPA and Rome Laboratories.

The authors are with the Electrical and Computer Engineering Department, University of California at Santa Barbara, Santa Barbara, CA 93106 USA.

Publisher Item Identifier S 0733-8724(96)08922-0.

sitics, and avalanche buildup time on the frequency response are included, and the effect of hole trapping at the heterointerface can be easily incorporated into the analysis depending on the type of the multiplying charge. Both front- and back-illumination are considered. Previous expressions given in [12] are a special case of this treatment.

This paper is organized as follows. Section II will discuss the effect of electric field profile on the performance of an APD. It will then be clear why a structure with peak electric field near the interface of absorption and multiplication layers is superior to that with a peak electric field near the edge of depletion layer. In Section III, we present an analysis of frequency response of a SAM–APD, taking into account the contribution from the secondary multiplying charges. In Section IV, we use the formula to calculate the bandwidth and gain-bandwidth product for SHIP's, and compare it to the data from our primary measurement of a SHIP detector. Performance of a SHIP detectors with various parameters will be predicted. Finally, in Section V, conclusions will be presented.

II. Effect of Electric Field Profile on Avalanche Buildup Time

It is well known that the ionization coefficients of semiconductors are functions of electric field. Given electron ionization coefficient α and hole ionization coefficient β, the multiplication gain for electrons M_e can be expressed as [18]

$$M_e = \left[1 - \int_0^{w_m} \alpha \exp\left(-\int_0^x [\alpha(x') - \beta(x')]dx'\right)dx\right]^{-1} \tag{1}$$

where w_m is the thickness of the multiplication layer. This expression is valid for pure electron injection from $x = 0$. For a uniform electric field profile, the above expression of M_e reduces to a simpler form [18]

$$M_e = \frac{(\alpha - \beta)\exp[(\alpha - \beta)w_m]}{\alpha - \beta\exp[(\alpha - \beta)w_m]}. \tag{2}$$

For silicon, the major multiplying charge is electron because α is 50 to 100 times larger than β. At higher electric fields, the ratio β/α becomes larger, resulting in larger excess noise factors [8], [19] as well a larger avalanche buildup times [15]. For a uniform electric field and equal saturation velocities, the avalanche buildup time, $\tau = M_e\tau_m$, is related to the ratio of the ionization coefficients by the following expression of the intrinsic response time τ_m [15]:

$$\tau_m = \kappa_1 \frac{\beta}{\alpha}\frac{w_m}{v} \tag{3}$$

where κ_1 is a correction factor which slowly varies with the ratio β/α [15], and v is the saturation velocity in avalanche region. For a nonuniform electric field profile, τ_m must be calculated by the following expression [20], [21]:

$$\tau_m = \frac{1}{v_n + v_p}\int_0^{w_m} \kappa_2 \exp\left[-\int_0^x [\alpha(x') - \beta(x')]dx'\right]dx \tag{4}$$

where κ_2 is another correction factor which varies with the ratio β/α and the ratio of the saturation velocities [21]. It can be easily shown that a uniform electric field profile is inferior to some other simple profiles. Referring to Fig. 2, we compare a uniform profile to a piece-wise uniform profile with two segments, for simplicity. Using Grant's ionization coefficients for silicon [18], we obtain that the electric field required to achieve high gain (close to breakdown) with an 0.5 μm thick avalanche layer is $E_{\text{uni}} = 373$ kV/cm. For a two-segment piecewise uniform profile, the required electric field is dependent on the direction in which electrons are injected. Assume that the electric fields for the lower portion of the profile are the same, say, $E_{\text{low}} = 273$ kV/cm. If the electrons are injected from the higher electric field side, then the electric field for the higher segment required to achieve high gain is $E_{\text{hi1}} = 427$ kV/cm. On the other hand, if electrons are injected from the other side, then the electric field for the higher segment will be $E_{\text{hi2}} = 445$ kV/cm to achieve high gain. The reason that the piece-wise uniform profile with its higher segment facing the injected electrons is better than the uniform profile can be explained as follows. First, the voltage needed to deplete the multiplication layer is smaller. Second, the effective multiplication plane is shifted toward the absorption layer. Therefore, the effective transit time for the secondary charges will be smaller, resulting in a larger bandwidth for transit time limited APD's. Third, according to (4), the effective avalanche buildup time is smaller, resulting a large gain-bandwidth product. From a practical point of view, this is very important in designing a high-speed APD. Generally speaking, an electric field profile with its peak close to the absorption layer is desirable. Fig. 3 shows the electric field profile of a SHIP detector without the intrinsic Si layer (see Fig. 1). Note that for this structure, the peak electric field is not at the edge of the depletion layer. Instead, it is close to the heterointerface of the multiplication layer and the absorption layer. Such an electric field profile is quite different from the model that was used in InP/InGaAs APD's [12]. As a consequence, the frequency response of this type of APD will be different from that derived previously. For this type of electric field profile, as well as other profiles whose effective multiplication plane not located at the edge of the depletion layer, a new theory of the frequency response is needed.

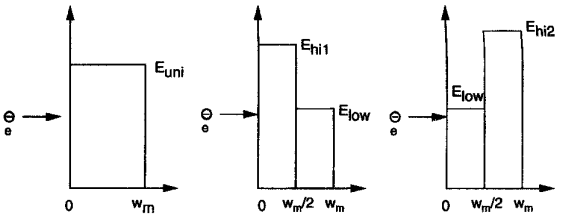

Fig. 2. Comparison among (a) a uniform electric field profile, (b) a two-segment piece-wise uniform electric field profile with electrons injected from the higher field segment, and (c) a two-segment piece-wise uniform electric field profile with electrons injected from the lower field segment, for a 0.5 μm thick multiplication layer. Case (b) is most desirable because of its smallest operating voltage (the area under the profile), smallest avalanche buildup time [estimated using (4)], and the smallest Δw_m.

III. Frequency Response of SAM-APD's

The frequency response is a very important measure for APD's because of their application in high bit-rate communi-

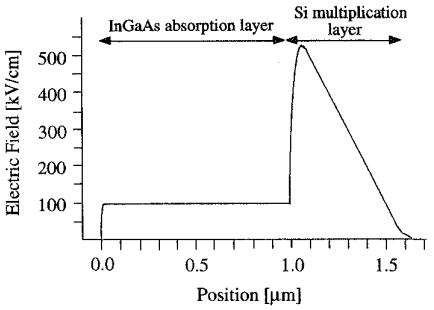

Fig. 3. Calculated electric field profile of a SHIP detector biased near operating voltage. The detector structure consists of a 6×10^{16} cm^{-3} n-type doped silicon wafer implanted with a 3.5×10^{12} cm^{-2} dose of 10 keV boron atoms. Attached to the silicon is a 1.0 μmthick intrinsic InGaAs layer and a thin p^+ InGaAs layer for ohmic contact.

cation systems. In designing and optimizing a SAM–APD, it is necessary to calculate the frequency response for given device parameters. Earliest treatment of the frequency response of SAM–APD's assumed that the effects of transit time, high-gain roll-off due to avalanche buildup time, and hole trapping at the heterointerface are all independent of each other. As a result, the frequency response was expressed as a product of terms, each representing one of the effects [11]. In reality, however, these effects are not independent of each other. More recently, Campbell *et al.* [12] presented an expression for the frequency response of InP/InGaAs APD's. However,, the contribution of the secondary holes to the frequency response was ignored. Such an approximation is only true when it can be reasonably assumed that all the secondary charges are generated at the edge of the depletion layer. This assumption was partly justified in that treatment because the electric field profile was triangular with its peak located at the edge of the depletion layer (interface of p^+/p-InP). As a result, multiplication took place near the peak field and the secondary holes were collected right after they were generated and their contribution to the impulse response could be neglected. Although this assumption may be a good one for that particular structure, it does not apply to other structures where the peak electric field is not at the edge of the depletion layer. For SHIP detectors, as well as other SAM-APD's with different electric field profiles, we can no longer neglect the contribution of the secondary major multiplying charges (holes for InP and electrons for Si) to the frequency response of the APD's. The effect of the transit time of these secondary multiplying charges on the frequency response becomes more important when the thickness of the multiplication layer becomes larger. Hence, a model taking into account the contribution of secondary multiplying charges to the frequency response is needed for analyzing more precisely the performance of these APD's. In what follows, we present the analytical expressions of frequency response for SAM-APD's, taking into account the contribution from the secondary multiplying charges. The notation is based on the assumption that electrons are the major multiplying charges. Hole trapping at the hetero-interface is not considered till the next section so that these expressions can be used for hole-multiplying APD's with minor modifications.

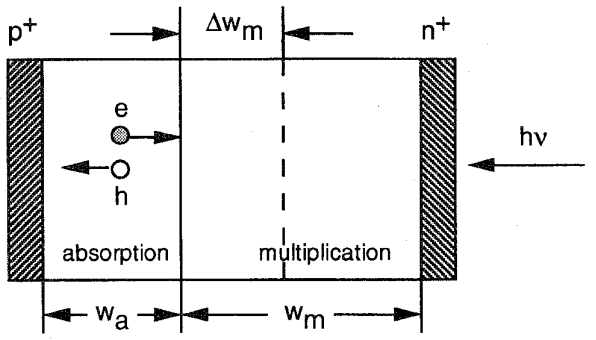

Fig. 4. One-dimensional model of a SAM–APD.

Referring to Fig. 4, we assume that the thickness of the absorption layer is w_a and that of the multiplication layer is w_m. We assume that all the secondary charges are generated at the same plane (the effective multiplication plane) inside the multiplication layer. In this theory, this plane is located from the interface of the absorption layer and the multiplication layer by a distance of Δw_m. We further assume that the APD is back-illuminated from the side of the multiplication layer, as shown in Fig. 4. In addition, we assume that both the absorption layer and the multiplication layer are fully depleted such that the thickness of the depletion layer is simply given by $w_d = w_a + w_m$. In this case, the photocurrent can be written as

$$i_{\rm ph}(t) = \frac{q}{w_d}[v_n N(t) + v_p P(t) + v_n N_s(t) + v_p P_s(t)] \quad (5)$$

where q is the electronic charge, v_n and v_p are the electron and hole saturated drift velocities, and $N(t), P(t), N_s(t)$, and $P_s(t)$ are the total number of uncollected photogenerated primary electrons, primary holes, secondary electrons, and secondary holes in the depletion region, respectively. In the frequency domain, the signal current read through the load resistor can be expressed as

$$i_s(\omega) = \frac{q}{w_d}\frac{v_n\tilde{N}(\omega) + v_n\tilde{N}_s(\omega) + v_p\tilde{P}(\omega) + v_p\tilde{P}_s(\omega)}{1 - \omega^2 LC + j\omega C(R_s + R_l)} \quad (6)$$

where L is the parasitic inductance, C is the total capacitance of the APD, R_s is the series resistance, R_l is the load resistance, and $\tilde{N}(\omega), \tilde{P}(\omega), \tilde{N}_s(\omega)$, and $\tilde{P}_s(\omega)$ are the Fourier transforms of $N(t), P(t), N_s(t)$, and $P_s(t)$, respectively.

To calculate the frequency response, we take the Fourier transform of $N(t), P(t), N_s(t)$, and $P_s(t)$ generated by an input optical impulse [21]. The impulse response for an APD with a structure shown in Fig. 4 illuminated from the multiplication layer is given by

$$\begin{aligned} N(t) =& \frac{\eta P_0}{h\nu}[1 - \exp(-\alpha w_a)][u(t) - u(t - t_2)] \\ &+ [\exp(-\alpha v_n(t - t_2)) - \exp(-\alpha w_a)] \\ &\times [u(t - t_2) - u(t - t_2 - t_3)] \quad (7) \\ P(t) =& \frac{\eta P_0}{h\nu}[1 - \exp(\alpha v_p(t - t_4))][u(t) - u(t - t_4)] \quad (8) \end{aligned}$$

$$\frac{P_s(t)}{M_0-1} = \left\{ \frac{\eta P_0}{h\nu}[1-\exp(-\alpha v_n(t-t_1))] \times [u(t-t_1)-u(t-t_1-t_3)] + \frac{\eta P_0}{h\nu}[1-\exp(-\alpha w_a)] \times [u(t-t_1-t_3)-u(t-t_5)] + \frac{\eta P_0}{h\nu}[\exp(-\alpha v_n(t-t_5))-\exp(-\alpha w_a)] \times [u(t-t_5)-u(t-t_3-t_5)] \right\} \otimes \frac{\exp[-t/(M_0-1)\tau_m]}{(M_0-1)\tau_m} \tag{9}$$

$$\frac{N_s(t)}{M_0-1} = \left\{ \frac{\eta P_0}{h\nu}[1-\exp(-\alpha v_n(t-t_1))] \times [u(t-t_1)-u(t-t_2)] + \frac{\eta P_0}{h\nu}[\exp(-\alpha v_n(t-t_2))-\exp(-\alpha v_n(t-t_1))] \times [u(t-t_2)-u(t-t_1-t_3)] \right\} + \left\{ \frac{\eta P_0}{h\nu}[\exp(-\alpha v_n(t-t_2))-\exp(-\alpha w_a)] \times [u(t-t_1-t_3)-u(t-t_2-t_3)] \right\} \otimes \frac{\exp[-t/(M_0-1)\tau_m]}{(M_0-1)\tau_m} \tag{10}$$

$$(w_m < w_a + 2\Delta w_m)$$

or

$$\frac{N_s(t)}{M_0-1} = \left\{ \frac{\eta P_0}{h\nu}[1-\exp(-\alpha v_n(t-t_1))] \times [u(t-t_1)-u(t-t_1-t_3)] + \frac{\eta P_0}{h\nu}[1-\exp(-\alpha w_a)][u(t-t_1-t_3)-u(t-t_2)] \right\} + \left\{ \frac{\eta P_0}{h\nu}[\exp(-\alpha v_n(t-t_2))-\exp(-\alpha w_a)] \times [u(t-t_2)-u(t-t_2-t_3)] \right\} \otimes \frac{\exp[-t/(M_0-1)\tau_m]}{(M_0-1)\tau_m} \tag{11}$$

$$(w_m \geq w_a + 2\Delta w_m)$$

where $t_1 = \Delta w_m/v_n, t_2 = w_m/v_n, t_3 = w_a/v_n, t_4 = w_a/v_p, t_5 = w_a/v_p + \Delta w_m/v_n + \Delta w_m/v_p$, P_0 is the energy of the optical impulse, $h\nu$ is the photon energy, η is the external quantum efficiency, α is the absorption coefficient, M_0 is the dc gain of the APD, τ_m is the avalanche buildup time constant of the APD, and $\otimes$ stands for the convolution operation. In deriving the expressions for the secondary charges, we have assumed that the multiplication takes place at the plane which is Δw_m away from the interface, as shown in Fig. 4.

The impulse response is broadened by the multiplication process as indicated by the convolution operation. Note that the impulse responses are piece-wise functions with each segment describing the generation, drift, and/or reduction of the photocarries in the depletion region. The physical meaning of each term of the impulse responses is clear. For example, the first term in $N(t)$ represents the drift of the electrons from the absorption region to the multiplication region, while the second term represents the reduction of the electrons due to collection at the edge of the multiplication layer. Similarly, the first term of $P_s(t)$ represents the generation of the secondary holes; the second term represents the drift of all the secondary holes; and the third term represents the reduction of the secondary holes due to the collection at the edge of the absorption layer. It is worth noting that mathematically (10) and (11) are equivalent regardless of the magnitudes of w_m and w_a, although the physical meaning of each corresponding term is different. The impulse responses (7)–(10) are qualitatively illustrated in Fig. 5.

The Fourier transforms of the impulse responses are given by

$$\tilde{N}(\omega) = \frac{\eta P_0}{h\nu}\left[\frac{1-\exp(-\alpha w_a)}{j\omega} + \exp(-j\omega w_m/v_n) \times [1-\exp(-\alpha w_a - j\omega w_a/v_n)]\left(\frac{1}{j\omega+\alpha v_n} - \frac{1}{j\omega}\right)\right] \tag{12}$$

$$\tilde{P}(\omega) = \int_0^{w_a/v_n} \frac{\eta P_0}{h\nu}[1-\exp(-\alpha w_a + \alpha v_p t)]\exp(-j\omega t)dt = \frac{\eta P_0}{h\nu}\left[\frac{1-\exp(-j\omega w_a/v_p)}{j\omega} + \frac{\exp(-j\omega w_a/v_p)-\exp(-\alpha w_a)}{j\omega - \alpha v_p}\right] \tag{13}$$

$$\frac{\tilde{P}_s(\omega)}{M_0-1} = \frac{\eta P_0}{h\nu}\exp(-j\omega\Delta w_m/v_n)[1-\exp(-\alpha w_a - j\omega w_a/v_n)] \times [1-\exp(-j\omega(w_a+\Delta w_m)/v_p)] \times \left(\frac{1}{j\omega} - \frac{1}{j\omega+\alpha v_n}\right)\frac{1}{1+j\omega(M_0-1)\tau_m} \tag{14}$$

$$\frac{\tilde{N}_s(\omega)}{M_0-1} = \frac{\eta P_0}{h\nu}\exp(-j\omega\Delta w_m/v_n)[1-\exp(-\alpha w_a - j\omega w_a/v_n)] \times [1-\exp(-j\omega(w_m-\Delta w_m)/v_n)] \times \left(\frac{1}{j\omega} - \frac{1}{j\omega+\alpha v_n}\right)\frac{1}{1+j\omega(M_0-1)\tau_m}. \tag{15}$$

The Fourier transform of (11) is the same as (15), as we expect.

From (6), it can be shown that the dc photocurrent is equal to the gain times the number of photoinduced electron-hole

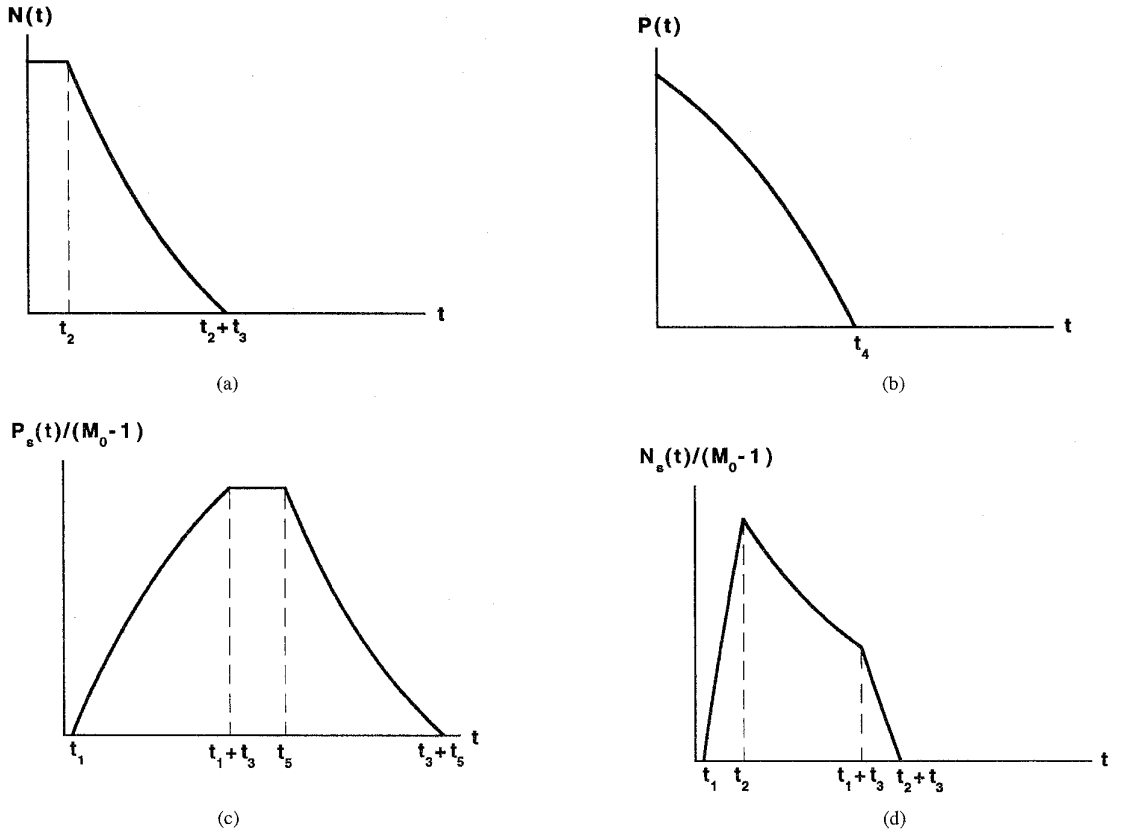

Fig. 5. Impulse response of a SAM-APD for (a) primary electrons, (b) primary holes, (c) secondary holes, and (d) secondary electrons.

pairs

$$i_s(\omega=0)=\frac{q}{w_d}[v_n\tilde{N}(0)+v_n\tilde{N}_s(0)+v_p\tilde{P}(0)+v_p\tilde{P}_s(0)]$$
$$=\int_0^\infty i_{\rm ph}(t)dt=\frac{q\eta P_0}{h\nu}M_0[1-\exp(-\alpha w_a)] \tag{16}$$

The frequency response, which is usually expressed as the ratio of the signal current to the dc current, can be written as

$$\frac{i_s(\omega)}{i_s(0)}=\frac{h\nu}{\eta P_0 M_0[1-\exp(-\alpha w_a)]}\times\frac{1}{1-\omega^2LC+j\omega RC}$$
$$\times\frac{1}{w_d}[v_n\tilde{N}(\omega)+v_n\tilde{N}_s(\omega)+v_p\tilde{P}(\omega)+v_p\tilde{P}_s(\omega)]. \tag{17}$$

Equation (17) gives the frequency response for a SAM–APD in which multiplication takes place at a plane located Δw_m away from the interface of the absorption layer and the multiplication layer. When we set $\Delta w_m = w_m$, (12)–(15) then reduce to the expressions obtained by Campbell *et al.* [12]. By setting $\Delta w_m = 0$, we have the expressions for the frequency response of an APD in which multiplication takes place at the interface. In addition, (17) can be easily generalized to SAM-APD's with a "grading" layer. The presence of such a grading layer is equivalent to an increase in Δw_m. By properly choosing the value of Δw_m, the effects of electric field profile and/or grading layer can be taken into account. Note that in deriving (17), the effect of hole trapping at the hetero-interface has been neglected. The reason for this is to keep the expressions of the frequency response valid for both cases of APD's with either electron multiplication or hole multiplication. For SAM–APD's with hole multiplication, we only need to interchange P and N, as well as the p and n subscripts in (7)–(15). For an APD with a properly designed grading layer, hole trapping may be reasonably neglected. If this is not the case, then the effect of hole trapping can be treated as in [12] by the use of an effective emission rate of holes at the heterointerface, e_h. For APD's with hole multiplication, it is exactly the same as the case treated in [12], i.e., the drift term of the primary holes should be modified accordingly. Therefore, $\tilde{P}(\omega)$ should be modified *to*

$$\tilde{P}(\omega)$$
$$=\frac{\eta P_0}{h\nu}\left[\frac{1-\exp(-\alpha w_a)}{j\omega}+\frac{j\omega/e_h+\exp(-j\omega w_m/v_n)}{1+j\omega/e_h}\right.$$
$$\left.\times\,[1-\exp(-\alpha w_a-j\omega w_a/v_n)]\left(\frac{1}{j\omega+\alpha v_n}-\frac{1}{j\omega}\right)\right] \tag{18}$$

and both $\tilde{P}_s(\omega)$ and $\tilde{N}_s(\omega)$ should be multiplied by the factor $1/(1+j\omega/e_h)$. For APD's with electron multiplication, $\tilde{N}_s(\omega)$

and $\tilde{P}(\omega)$ are not affected, but $\tilde{P}_s(\omega)$ should be modified to

$$\frac{\tilde{P}_s(\omega)}{M_0-1} = \frac{\eta P_0}{h\nu}\exp(-j\omega\Delta w_m/v_n)[1-\exp(-\alpha w_a - j\omega w_a/v_n)] \times \left[1-\exp(-j\omega\Delta w_m/v_p)\frac{j\omega/e_h+\exp(-j\omega w_a/v_p)}{1+j\omega/e_h}\right] \times \left(\frac{1}{j\omega}-\frac{1}{j\omega+\alpha v_n}\right)\times\frac{1}{1+j\omega(M_0-1)\tau_m}. \quad (19)$$

Electron trapping at the interface, on the other hand, is either absent or can be reasonably neglected due to the fact that the electron effective mass on the injection side is about 20 times smaller than the hole effective mass.

Another consideration in the frequency response of SAM–APD's is the direction of illumination light. Equation (17) is derived under the assumption that the APD is illuminated from the multiplication layer. For APD's with light incident from the absorption layer, the impulse response is given by

$$N(t) = \frac{\eta P_0}{h\nu}[1-\exp(-\alpha w_a)][u(t)-u(t-t_2)] + \frac{\eta P_0}{h\nu}[1-\exp(\alpha v_n(t-t_2-t_3))] \times [u(t-t_2)-u(t-t_2-t_3)] \quad (20)$$

$$P(t) = \frac{\eta P_0}{h\nu}[\exp(-\alpha v_p t)-\exp(-\alpha w_a)][u(t)-u(t-t_4)] \quad (21)$$

$$\frac{P_s(t)}{M_0-1} = \left\{\frac{\eta P_0}{h\nu}\exp(-\alpha w_a)[\exp(\alpha v_n(t-t_1))-1] \times [u(t-t_1)-u(t-t_1-t_3)] + \frac{\eta P_0}{h\nu}[1-\exp(-\alpha w_a)][u(t-t_1-t_3)-u(t-t_5)] + \frac{\eta P_0}{h\nu}[1-\exp(\alpha v_n(t-t_3-t_5))] \times [u(t-t_5)-u(t-t_3-t_5)]\right\} \otimes \frac{\exp[-t/(M_0-1)\tau_m]}{(M_0-1)\tau_m} \quad (22)$$

$$\frac{N_s(t)}{M_0-1} = \left\{\frac{\eta P_0}{h\nu}\exp(-\alpha w_a)[\exp(\alpha v_n(t-t_1))-1] \times [u(t-t_1)-u(t-t_2)] + \frac{\eta P_0}{h\nu}\exp(-\alpha w_a) \times [\exp(\alpha v_n(t-t_1))-\exp(\alpha v_n(t-t_2))] \times [u(t-t_2)-u(t-t_1-t_3)]\right\} + \left\{\frac{\eta P_0}{h\nu}[1-\exp(\alpha v_n(t-t_2-t_3))] \times [u(t-t_1-t_3)-u(t-t_2-t_3)]\right\} \otimes \frac{\exp[-t/(M_0-1)\tau_m]}{(M_0-1)\tau_m}. \quad (23)$$

The Fourier transforms of (20)–(23) are given by

$$\tilde{N}(\omega) = \frac{\eta P_0}{h\nu}\left[\frac{1-\exp(-\alpha w_a)}{j\omega}-\exp(-j\omega w_m/v_n) \times [\exp(-\alpha w_a)-\exp(-j\omega w_a/v_n)] \times\left(\frac{1}{j\omega}-\frac{1}{j\omega-\alpha v_n}\right)\right] \quad (24)$$

$$\tilde{P}(\omega) = \frac{\eta P_0}{h\nu}\left[\frac{1-\exp(-j\omega w_a/v_p-\alpha w_a)}{j\omega+\alpha v_p} - \frac{1-\exp(-j\omega w_a/v_p)}{j\omega}\right] \quad (25)$$

$$\frac{\tilde{P}_s(\omega)}{M_0-1} = \frac{\eta P_0}{h\nu}\exp(-j\omega\Delta w_m/v_n) \times [\exp(-\alpha w_a)-\exp(-j\omega w_a/v_n)] \times [1-\exp(-j\omega(w_a+\Delta w_m)/v_p)] \times \left(\frac{1}{j\omega-\alpha v_n}-\frac{1}{j\omega}\right)\frac{1}{1+j\omega(M_0-1)\tau_m} \quad (26)$$

$$\frac{\tilde{N}_s(\omega)}{M_0-1} = \frac{\eta P_0}{h\nu}\exp(-j\omega\Delta w_m/v_n) \times [\exp(-\alpha w_a)-\exp(-j\omega w_a/v_n)] \times [1-\exp(-j\omega(w_m-\Delta w_m)/v_n)] \times \left(\frac{1}{j\omega-\alpha v_n}-\frac{1}{j\omega}\right)\frac{1}{1+j\omega(M_0-1)\tau_m}. \quad (27)$$

With (24)–(27), the frequency response of an APD illuminated from the absorption layer can be easily obtained by using (17). Again, for hole multiplying APD's, P and N, as well as the subscripts p and n in (20)–(27) should be interchanged. It can be shown that in the limiting case of $\alpha w_a \ll 1$, (24)–(27) are the same as (12)–(15). On the other hand, if $\alpha w_a \gg 1$, then illumination from different directions can make a significant difference to the frequency response.

As a comparison of this theory to the previous theory with the assumption of $\Delta w_m = w_m$, we now calculate the frequency response for a SAM–APD with the structure shown in Fig. 4. The parameters used in our calculation are $w_a = 1\ \mu$m, $w_m = 0.5\ \mu$m, $\Delta w_m = 0$, dc gain $M_0 = 10$, and absorption coefficient $\alpha = 1.15\ \mu\text{m}^{-1}$. The total resistance and capacitance are assumed to be 60 Ω and 0.1 pF, respectively. The inductance is assumed to be small enough so that it is neglected here. The saturation velocities of holes and electrons are 4.8×10^6 cm/s and 7.0×10^6 cm/s, respectively, corresponding to InGaAs. As we can see from Fig. 6, the difference in 3 dB bandwidth predicted by our theory and the previous theories is significant for this case even when w_m is still much smaller than w_a.

IV. Frequency Response of SHIP Detectors

The expressions for the frequency response of SAM–APD's derived in the previous section can be used to analyze the performance of SHIP detectors. The electron and hole ionization coefficients are also required to determine the frequency

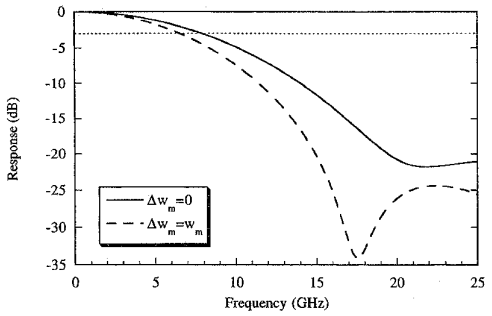

Fig. 6. Frequency response of a SAM–APD with $w_m = 0.5$ μm and $w_a = 2$ μm. Solid lines shows the result obtained using this theory with $\Delta w_m = 0$, while the dashed line shows the results obtained with $\Delta w_m = w_m$.

response of the SHIP's. These ionization coefficients vary with electric field and experiments to determine these coefficients by measuring carrier multiplication have yielded widely different results, especially at high electric fields [18], [23], [24]. The APD's used to make these measurements utilized the same region for multiplication and absorption and a very exact knowledge of electric field profiles and device structures are required to make an accurate determination of ionization coefficients. This have turned out to be very difficult to achieve as we can see from the discrepancies presented in the previous measurements. Fortunately, as far as the gain-bandwidth product is concerned, only the ratio of the ionization coefficients [cf., (3)–(4)] needs to be determined. The ratio of the ionization coefficients can be determined more accurately by measuring the excess noise of an APD versus multiplication gain [4]. Kaneda [25] did measurements of the ratio in silicon using a "reach through" structure [26] similar to a SAM APD. This method should be much more accurate at high electric fields. According to the measurements by Kaneda, the ratio of the ionization coefficients in silicon as a function of the thickness of the multiplication layer can be expressed as [25] $k_{\text{eff}}(w_m) = 0.22k_{\text{Grant}}(w_m)$ where $k_{\text{Grant}}(w_m)$ is the ratio obtained by using Grant's ionization coefficients for a given thickness of the multiplication layer. The ratio of the ionization coefficients obtained from Kaneda's experiment should be more applicable in computing the frequency response of the SHIP's because the measurement is based on a similar APD structure and were derived from values accurate at high electric fields.

Using the analytical expressions for the frequency response derived in the previous section and the ratio of the ionization coefficients in silicon, we calculate the 3 dB bandwidth of a SHIP detector. The parameters for the SHIP detector are $R = 2020\ \Omega, C = 0.1$ pF, $w_m = 2.5$ μm, $w_a = 1$ μm, and absorption coefficient $\alpha = 1.15$ μm^{-1}. The structure of this APD requires our newly derived theory be employed in analyzing its frequency response. This is because the thickness of the SHIP detector is so large that it can no longer be neglected compared to that of the absorption layer. In addition, due to the presence of the implanted p^+ layer at the interface of i-Si/i-InGaAs, the peak electric field is located at the interface instead of the edge of the depletion layer, as shown in Fig. 3.

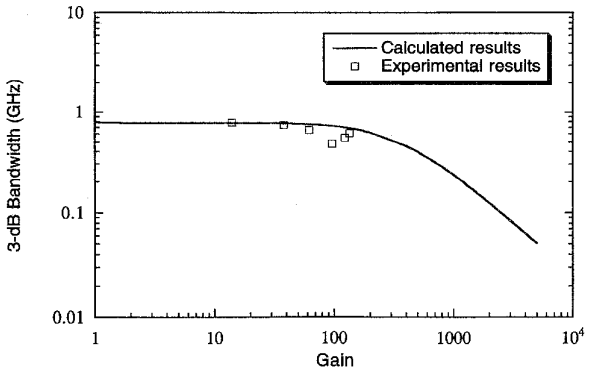

Fig. 7. A 3 dB bandwidth as a function of the multiplication gain for a SHIP detector with $w_a = 1$ μm, $w_m = 2.5$ μm. The resistance and the capacitance of the SHIP detector are 2020 Ω and 0.1 pF, respectively. The experimental data points are also shown in the figure.

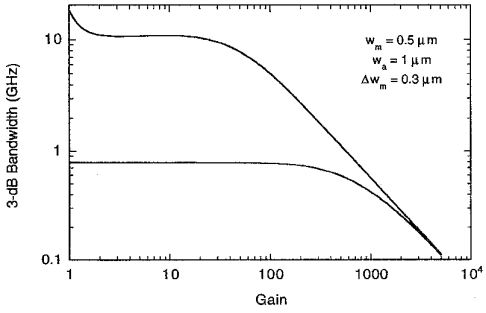

Fig. 8. 3 dB bandwidth as functions of the multiplication gain for optimized SHIP detectors with gain-bandwidth greater than 500 GHz. The thickness of the multiplication layer is 0.5 μm, and the thickness of the absorption layer is 1 μm. The solid line is for the case of $R = 60\ \Omega$, while the dashed line is for the case of $R = 2020\ \Omega$.

Therefore, we can no longer assume that all the multiplication takes place at the edge of the depletion layer. Consequently, the contribution to the frequency response from both the secondary electrons and the secondary holes must be taken into account. In Fig. 7, the 3 dB bandwidth is plotted for the SHIP detector as a function of the multiplication gain. The calculated results are in agreement with the measured results for the SHIP detector [5].

The performance of SHIP detectors can be optimized by changing the thickness of the multiplication layer and/or the electric field profile. Fig. 8 shows the 3 dB bandwidth vs. multiplication gain for a SHIP detector with $w_a = 1$ μm, $w_m = 0.5$ μm and $\Delta w_m = 0.3$ μm for $R = 2020\ \Omega$ and $R = 60\ \Omega$. To achieve a 10 GHz bandwidth ceiling at low gain region, the resistance of the SHIP detector should be reduced to 60 Ω. The gain-bandwidth product constants at high gain region for both cases are about 550 GHz. This gain-bandwidth product is five times higher than is expected or measured for InGaAs/InP APD's, and indicates the potential of SHIP detectors.

V. Conclusion

In conclusion, we have presented a theoretical analysis on the frequency response of SAM–APD's taking into account

the effects of parasitics, transit time, and avalanche buildup time. For the first time, we have considered the effect of electric field profile in the multiplication layer on the frequency response. Previous expressions of the frequency response can be regarded as special cases of this theory. We have compared the calculated results to the experimental results obtained from the measurement of a SHIP detector. We have also shown that an optimized SHIP detector can exhibit a gain-bandwidth product larger than 500 GHz.

ACKNOWLEDGMENT

The authors would like to thank R. J. McIntyre for useful discussions.

REFERENCES

[1] B. L. Kasper and J. C. Campbell, "Multigigabit-per-second avalanche photodiode lightwave receivers," *J. Lightwave Technol.*, vol. LT-5, pp. 1351–1364, 1987.

[2] J. C. Campbell, "Heterojunction photodetectors for optical communications," *Heterostructures and Quantum Devices*. New York: Academic, 1994, pp. 243–271.

[3] S. Fujita, N. Henmi, I. Takano, M. Yamaguchi, T. Torikai, T. Suzaki, S. Takano, H. Ishihara, and M. Shikada, "A 10 Gbit/s 80 km optical fiber transmission experiment using a directly modulated DFB-LD and a high speed InGaAs APD," in *Tech. Dig. OFC'88*, New Orleans, LA, postdeadline paper, 1988.

[4] R. G. Smith and S. R. Forrest, "Sensitivity of avalanche photodetector receivers for long-wavelength optical communications," *Bell Syst. Tech. J.*, vol. 61, pp. 2929–2946, 1982.

[5] A. R. Hawkins, T. E. Reynolds, D. R. England, D. I. Babic, M. J. Mondry, K. Streubel, and J. E. Bowers, "Silicon hetero-interface photodetector," *Appl. Phys. Lett.*, vol. 68, pp. 3692–3694, 1996.

[6] T. P. Pearsall, "Impact ionization rates for electrons and holes in $Ga_{0.47}In_{0.53}As$," *Appl. Phys. Lett.*, vol. 36, pp. 218–220, 1980.

[7] L. W. Cook, G. E. Bulman, and G. E. Stillman, "Electron and hole impact ionization coefficients in GaAs," *Solid-State Electron.*, vol. 21, pp. 331–340, 1978.

[8] R. J. McIntyre, "Multiplication noise in uniform avalanche diodes," *IEEE Trans. Electron Dev.*, vol. ED-13, pp. 164–168, 1966.

[9] T. Kaneda, "Silicon and germanium avalanche photodiodes," *Semiconductors and Semimetals*. New York: Academic, vol. 22, 1985, pp. 263–289.

[10] K. Berchtold, O. Krumppholz, and J. Suri, "Avalanche photodetectors with a gain-bandwidth product of more than 200 GHz," *Appl. Phys. Lett.*, vol. 26, pp. 585–587, 1975.

[11] J. C. Campbell, W. S. Holden, G. J. Qua, and A. G. Dentai, "Frequency response of InP/InGaAsP/InGaAs avalanche photodiodes with separate absorption "grading" and multiplication regions," *IEEE J. Quantum Electron.*, vol. QE-21, pp. 1743–1746, 1985.

[12] J. C. Campbell, B. C. Johnson, G. J. Qua, and W. T. Tsang, "Frequency response of InP/InGaAsP/InGaAs avalanche photodetectors," *J. Lightwave Technol.*, vol. 7, pp. 778–784, 1989.

[13] S. R. Forrest, O. K. Kim, and R. G. Smith, "Optical response time of $In_{0.53}Ga_{0.47}As$/InP avalanche photodetectors," *Appl. Phys. Lett.*, vol. 41, pp. 95–98, 1982.

[14] R. J. McIntyre, "Factors affecting the ultimate capabilities of high speed avalanche photodetectors and a review of the state-of-the-art," in *Int. Electron Devices Meet. Tech. Dig.*, 1973, pp. 213–216.

[15] R. B. Emmons, "Avalanche-photodiode frequency response," *J. Appl. Phys.*, vol. 38, pp. 3705–3714, 1967.

[16] J. N. Hollenhorst, "Frequency response theory for multilayer photodiodes," *J. Lightwave Technol.*, vol. 8, pp. 531–537, 1990.

[17] G. Kahraman, B. E. A. Saleh, W. L. Sargeant, and M. C. Teich, "Time and frequency response of avalanche photodiodes with arbitrary structure," *IEEE Trans. Electron Devices*, vol. 39, pp. 553–560, 1992.

[18] W. N. Grant, "Electron and hole ionization rates in epitaxial silicon at high electric fields," *Solid-State Electron.*, vol. 16, pp. 1189–1203, 1973.

[19] J. C. Campbell, S. Chandrasekhar, W. T. Tsang, G. J. Qua, and B. C. Johnson, "Multiplication noise of wide-bandgap InP/InGaAsP/InGaAs avalanche photodiodes," *J. Lightwave Technol.*, vol. 7, pp. 473–477, 1989.

[20] R. Kuvas and C. A. Lee, "Quasistatic approximation for semiconductor avalanches," *J. Appl. Phys.*, vol. 41, pp. 1743–1755, 1970.

[21] I. M. Naqvi, "Effects of time dependence of multiplication process on avalanche noise," *Solid-State Electron.*, vol. 16, pp. 19–28, 1973.

[22] H. W. Ruegg, "An optimized avalanche photodiode," *IEEE Trans. Electron Dev.*, vol. ED-14, pp. 239–251, 1967.

[23] C. A. Lee, R. A. Logan, R. L. Batdorf, J. J. Kleimack, and W. Wiegmann, "Ionization rates of hole and electrons in silicon," *Phys. Rev.*, vol. 134, pp. A761–A773, 1964.

[24] P. P. Webb, "Measurements of ionization coefficients in silicon at low electric fields," presented at Electro-Optics Operations, GE Canada Inc.

[25] T. Kaneda, H. Matsumoto, and T. Yamaoka, "A model for reach-through avalanche photodiodes (RAPD's)," *J. Appl. Phys.*, vol. 47, pp. 3135–3139, 1976.

[26] R. J. McIntyre, "Recent developments in silicon avalanche photodiodes," *Measurement*, vol. 3, pp. 146–152, 1985.

Weishu Wu, photograph and biography not available at the time of publication.

Aaron R. Hawkins, photograph and biography not available at the time of publication.

John E. Bowers, photograph and biography not available at the time of publication.